JOURNAL OF SPACECRAFT AND ROCKETS
Vol. 38, No. 2, March–April 2001

Compressive Response of Lightweight Ceramic Ablators: Phenolic Impregnated Carbon Ablator

Kelly E. Parmenter,* Karl Shuman,† and Frederick Milstein‡
University of California, Santa Barbara, Santa Barbara, California 93106
and
Christine E. Szalai,§ Huy K. Tran,§ and Daniel J. Rasky¶
NASA Ames Research Center, Moffett Field, California 94035-1000

Lightweight ceramic ablators are porous fibrous ceramic substrates impregnated with organic resins. The materials were developed for use as heat shields for planetary entry. The compressive response and hardness of a phenolic impregnated carbon ablator and its fibrous substrates are reported. Results are also given for charred specimens of the ablator. Fibers in the substrate tend to be randomly and uniformly aligned parallel to a preferred plane. Two characteristic compressive responses were observed, depending on the orientation of the load with respect to the preferred fiber-alignment plane. When the load was parallel to this plane, the stress increased approximately linearly with increasing strain to strains of about 2%. The stress then followed an erratic "horizontal" path with increasing strain as the materials apparently failed by an internal separation and buckling mechanism. In contrast, during compression transverse to the fiber-alignment plane, the materials underwent significant, nonlinear, plastic deformation, wherein the stress increased with increasing strain to strains of over 50% without indications of fracture. Considerable energy was absorbed during compression, particularly for materials subjected to the transverse loading condition. Resin impregnation substantially strengthens the ablator material; this effect was prominent for specimens loaded transverse to the fiber-alignment plane.

Nomenclature

A	=	$\pi D\delta$, indentation surface area, mm^2
D	=	diameter of hardness indenter, mm
E_i	=	initial Young's modulus, MPa
$E_{X\%}$	=	secant modulus at $X\%$ of S, defined in Eq. (1), MPa
e	=	energy density, defined in Eq. (2), MJ/m^3
H	=	$L_{\max}/A$, hardness, MPa
$L_{\max}$	=	maximum load during hardness test, N
S	=	compressive strength, MPa
δ	=	depth of penetration of hardness indenter, mm
ε	=	strain, mm/mm
ε_S	=	strain at S, mm/mm
σ	=	stress, MPa
σ_Y	=	yield stress, MPa

Introduction

LIGHTWEIGHT ceramic ablators (LCAs) were developed by the Thermal Protection Materials and Systems Branch, at NASA Ames Research Center,[1] for use as heat shields on spacecraft intended for planetary missions. The materials must provide thermal protection of vehicle interiors and be capable of maintaining mechanical integrity while withstanding very high heating rates. LCAs consist of highly porous substrates of ceramic fibers that are partially impregnated with organic resins. The fibers in the substrates tend to lie parallel to a preferred plane; hence, the substrates and LCAs have anisotropic mechanical properties. To make effective use of LCAs in the design of heat shields and to manufacture LCAs with desired mechanical properties, it is important and necessary to determine the anisotropic mechanical responses of the materials under various conditions of load. Thus, we have instituted an ongoing program to characterize the mechanical responses of LCA composites. As part of this program, we have carried out an experimental study of the compressive behavior of phenolic impregnated carbon ablator, or PICA. PICA is important for applications where the heat fluxes are greater than about 400 W/cm^2. PICA was chosen as the heat shield for the Stardust Sample Return Capsule's forebody[2] and is a candidate for future sample return missions.

Tran et al.[1–5] and Chen and Milos[6] have measured the thermal performance and ablation characteristics of LCA materials, including PICA. Conditions encountered during atmospheric entry were simulated in the Ames Research Center's 60-MW Interaction Heating Facility and the 20-MW Aerodynamic Heating Facility. Under the conditions in these facilities, the LCAs ablate and develop a char layer that is on the order of a few millimeters thick. These tests have revealed that LCAs can withstand very high heating rates and surface pressures and are more efficient, per unit mass, than most traditional ablative materials. Recently, Marschall et al.[7,8] measured the gas permeability of PICA and its fibrous substrate material Fiberform®. They found that, when compared to the substrate material, the continuum permeability of virgin PICA was 15 to 25 times lower, and the continuum permeability for charred PICA was 8 to 12 times lower. Additionally, charring had a smaller effect on the permeability in the direction parallel to the plane of fiber alignment than in the transverse direction.

Although PICA has been subjected to extensive thermophysical testing, its mechanical properties have not heretofore been studied in a systematic manner. This paper presents the results of systematic compression and hardness testing of virgin and charred PICA. The mechanical properties of charred PICA are of particular interest because LCAs undergo charring during entry through planetary atmospheres. Additionally, to gain understanding of the basis for the composite's mechanical response, separate compression and hardness tests were made on the unimpregnated carbon fiber substrate, which, by itself, is capable of supporting significant compressive loads. To determine the anisotropy of the mechanical properties, the LCA and substrate materials were tested with uniaxial loads parallel to, and transverse to, the plane of preferred fiber alignment.

Received 9 June 2000; revision received 18 October 2000; accepted for publication 16 November 2000.

*Research Associate, Departments of Mechanical Engineering and Materials; kellyp@west.net.
†Research Assistant, Departments of Mechanical Engineering and Materials.
‡Professor, Departments of Mechanical Engineering and Materials; frdmlstn@engineering.ucsb.edu.
§Research Scientist, Thermal Protection Materials and Systems Branch. Member AIAA.
¶Senior Scientist, Thermal Protection Materials and Systems Branch. Member AIAA.

The next section of this paper describes the samples that were tested and the compression and hardness test procedures. The "Results" section then displays characteristic stress-strain responses, and compression and hardness results, for each type of material and loading condition. The penultimate section provides a discussion and comparison of the significant experimental findings, and the last section summarizes the important conclusions.

Materials and Test Procedures

Materials

Details of the development of PICA have been given by Tran.[1] PICA consists of a substrate of carbon fibers (14–16 μm diam) that is partially impregnated with the phenolic resin infiltrant Durite®, manufactured by Bordon Packaging and Industrial Products. The carbon-fiber substrate, called Fiberform, is manufactured by Fiber Materials, Inc. The density of Fiberform used in the present study ranged from 160 to 187 kg/m,[3] and the density of PICA ranged from 220 to 257 kg/m^3. The density of a given specimen is defined as its mass divided by its bulk volume, as determined by its exterior dimensions. To produce charred specimens for testing, samples of virgin PICA were pyrolyzed in a tube furnace at 1000°C for 10 min in an argon atmosphere, and then the furnace was turned off and the specimens were allowed to cool to room temperature, while remaining in the argon atmosphere. The cooling rate was approximately 50°C/min in the beginning and then tapered down to about 20°C/min toward the end. The pyrolysis process decomposes the resin infiltrants and yields fibrous substrates that are coated in a char residue. This procedure results in specimens that are uniformly charred throughout. The density of the charred PICA samples ranged from 213 to 225 kg/m^3. The range of density of the charred PICA samples prior to charring was 237 to 257 kg/m^3, and the range of density of the substrates was 165 to 167 kg/m^3. The typical mass loss during charring was 10–12%.

During processing of the fibrous substrates, the fibers tend to become aligned normal to a pressing direction. As a result, the fibers in the LCA composite naturally tend to be randomly and uniformly aligned parallel to a preferred plane. The term "parallel loading" or "parallel compression" is employed herein when the test load is applied parallel to the plane of preferred fiber alignment. Test loading perpendicular to the preferred plane is called "transverse loading" or "transverse compression" herein. Examples of the microstructure of PICA are shown in Fig. 1 at various levels of magnification. In Fig. 1 the plane of the images is coincident with the plane of preferred fiber alignment. Of course, the fibers are not all strictly parallel to the preferred plane. These photomicrographs show that the distribution of phenolic resin throughout the composite is not fully homogeneous. Coagulations of phenolic infiltrant appear evident as light colored regions in the lower right and upper left portions of Fig. 1d, which is at the lowest magnification. Regions of relatively sparse phenolic infiltrant are also evident as the darker regions between the fibers.

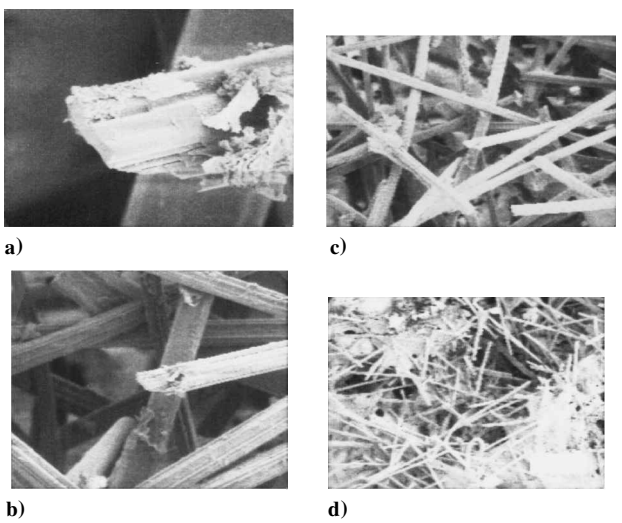

Fig. 1 Scanning electron photomicrographs, at four levels of magnification, of a region of the surface of a PICA specimen that was fractured in parallel loading. The fields have widths of approximately a) 25, b) 100, c) 250, and d) 750 μm.

Compression Tests

Specimens of PICA, charred PICA, and Fiberform for compression testing were cut into rectangular blocks of 2:1 height:width ratios with nominal dimensions of $12.7 \times 12.7 \times 25.4$ mm. Specimens for testing under transverse compression were cut with their long axis perpendicular to the preferred plane of fiber alignment, whereas those cut for parallel compression had their long axis parallel to the preferred plane. For both cases the direction of loading was parallel to the long axis. Each specimen was loaded in a displacement-controlled testing machine. The actual load was applied by means of a compression fixture, consisting of a flat plate on one side and a "frictionless" hemisphere, secured in a socket coated with vacuum grease, on the other side. With this arrangement the socket portion of the compression fixture was self-aligning. The load was measured with a compression load cell, and the crosshead displacement was measured with the testing machine's internal displacement gage. The displacements that were determined in this manner were checked against a laser extensometer and found to be accurate to within 1 μ over a 25.4-mm gage length. The crosshead speed ranged from about 0.10 to 0.76 mm/min, depending on the range of strain to be covered during the test. No noticeable effects of crosshead speed were observed in this range during testing. All tests were conducted under ambient conditions. For each specimen the load-displacement curve was converted to a stress-strain curve by dividing the measured loads by the specimen's original cross-sectional area and the measured displacements by the specimen's original height. Generally, compression tests were terminated after the load dropped to a point beyond which recovery to the maximum load would be unlikely. The compressive strength S was then taken to be the maximum compressive load that a specimen could support, divided by the original cross-sectional area of the specimen. The corresponding strain that occurs at this maximum load is denoted by ε_S.

Hardness Tests

Hardness testing of materials is widely used because it is relatively nondestructive, sample preparation and test procedures are usually uncomplicated, and correlations often exist between the hardness and other properties of interest. For example, relationships between strength and hardness are well known in metals and alloys. Kim and Milstein[9] also showed that such a relationship exists for polymer concrete materials, and Parmenter and Milstein[10] established a correlation between hardness and compressive strength for silica aerogels, including those that were fiber reinforced. Therefore, it is also desirable to determine to what extent the hardness of LCAs can be correlated with other mechanical properties.

Ordinary micro- and macrohardness tests on LCAs do not yield meaningful results. This shortcoming is because surface features, such as fibers and pores, are of the same order of size as microindenters, and loads for traditional macroindentation tests are too large. This circumstance was encountered previously by Parmenter and Milstein[10] in their studies of the mechanical properties of silica aerogels. To circumvent that problem, they employed a testing procedure that used low loads and a spherical indenter with a radius that is large compared to the material surface features. A similar procedure was used in the present study. A steel ball (19.05-mm diam) and socket fixture was secured to the crosshead of the displacement-controlled testing machine. The load was measured with a compression load cell, and the crosshead displacement was measured with a linear variable differential transformer. The crosshead speed was 0.102 mm/min. All tests were conducted under ambient conditions. An initial preload of 1.0 N was applied to establish a point of reference. The load was subsequently increased to a nominal value of 30 N and then reduced to the preload value where the depth of penetration δ was measured. Figure 2 depicts the depth δ on a load vs displacement curve for a typical hardness test. The indentation surface area A was approximated from the measured value of δ and ball diameter D with the relationship $A = \pi D\delta$. The hardness H was defined as the maximum load $L_{\max}$ divided by the indentation surface area, that is, $H = L_{\max}/A$.

Table 1 Compressive properties of PICA, charred PICA, and the fibrous substrate Fiberform in parallel loading[a]

Material	No. of specimens	Density, kg/m^3	S, MPa	ε_S, mm/mm	$E_{50\%}$, MPa	$E_{90\%}$, MPa
PICA	18	220 ± 4	1.55 ± 0.09	0.023 ± 0.011	143 ± 17	106 ± 9
Charred PICA	11	225 ± 8	1.79 ± 0.43	0.031 ± 0.006	107 ± 19	78 ± 21
Fiberform	10	187 ± 6	0.81 ± 0.08	0.041 ± 0.011	57 ± 12	32 ± 3

[a]The values following the $\pm$ are standard deviations.

Table 2 Compressive properties of PICA, charred PICA, and the fibrous substrate Fiberform in transverse loading[a]

Material	No. of specimens	Density, kg/m^3	S, MPa	ε_S, mm/mm	E_i, MPa	σ_Y, MPa
PICA	11	221 ± 2	5.46 ± 0.77	0.709 ± 0.018	12 ± 2	0.27 ± 0.06
Charred PICA	8	219 ± 4	3.54 ± 0.65	0.688 ± 0.042	33 ± 7	0.36 ± 0.05
Fiberform	12	185 ± 4	1.01 ± 0.02[b]	0.580 ± 0.003[b]	14 ± 1	0.17 ± 0.02

[a]The values following the $\pm$ are standard deviations.
[b]Average value was calculated from two tests.

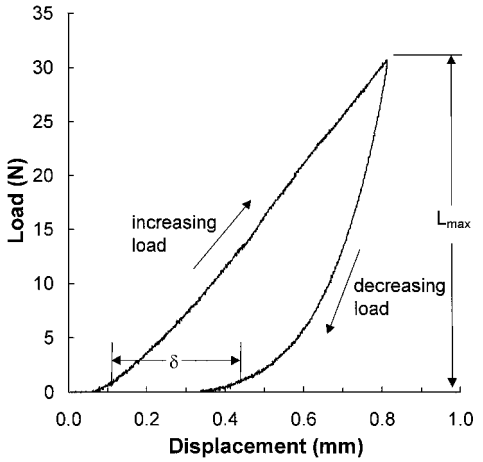

Fig. 2 Load vs displacement curve for a typical hardness test.

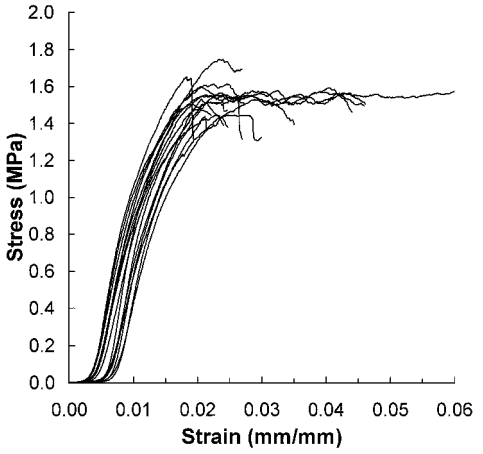

Fig. 3 Stress-strain curves obtained from parallel-compression testing of PICA (density = 220 ± 4 kg/m^3).

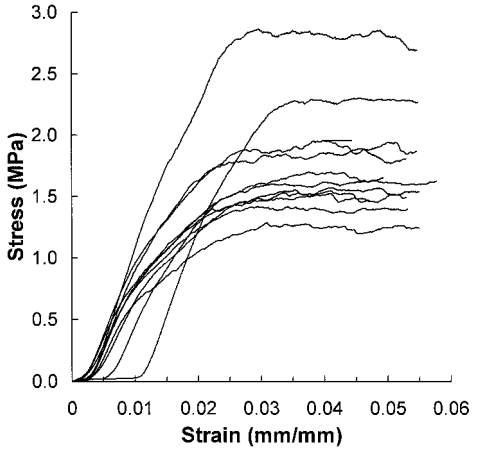

Fig. 4 Stress-strain curves obtained from parallel-compression testing of charred PICA (density = 225 ± 8 kg/m^3).

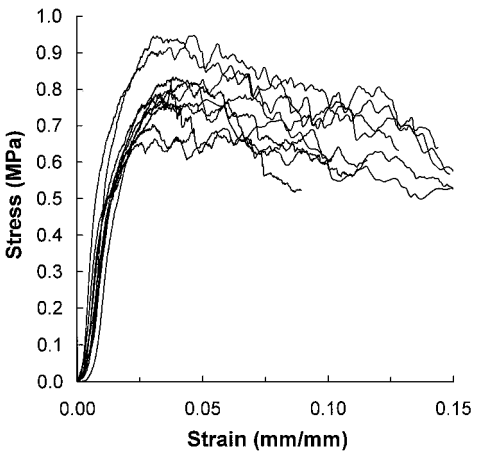

Fig. 5 Stress-strain curves obtained from parallel-compression testing of the Fiberform substrate (density = 187 ± 6 kg/m^3).

Results

Figures 3–5 show the responses of PICA, charred PICA, and Fiberform under parallel compressive loading, and Table 1 summarizes various mechanical properties derived from these plots. Each figure has multiple "curves," and each curve corresponds to the response of an individual specimen that was tested. Typically, macroscopic fracture of these specimens was not observed under parallel loading unless the strain far exceeded ε_S, the strain at the maximum stress, although indications of microscopic fracture appeared prior to achieving the maximum stress. In Table 1 the determinations of ε_S and the secant moduli $E_{50\%}$ and $E_{90\%}$ are reckoned to reference states at which the stress is 0.05 MPa to eliminate initial transient effects. The secant moduli are the slopes defined by

$$E_{X\%} = \frac{[\text{stress at } X\% \text{ of } S - 0.05 \text{ MPa}]}{[\text{strain at } X\% \text{ of } S - \text{strain at } 0.05 \text{ MPa}]} \tag{1}$$

where $X\%$ is either 50 or 90%. Thus, the moduli are a measure of the stiffness of material in parallel compression.

Figures 6–8 show the transverse compressive responses of PICA, charred PICA, and Fiberform, and Table 2 lists mechanical properties that correspond to these results. As in Figs. 3–5, each

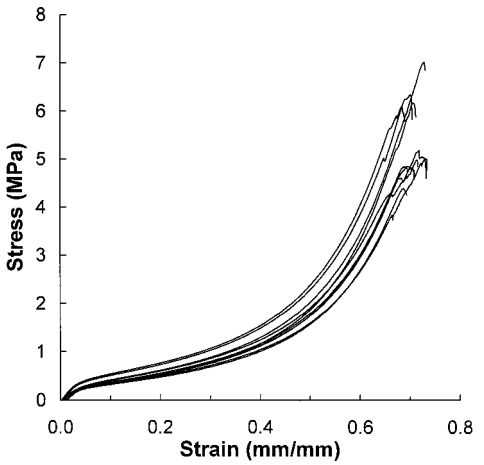

Fig. 6 Stress-strain curves obtained from transverse-compression testing of PICA (density = 221 ± 2 kg/m^3).

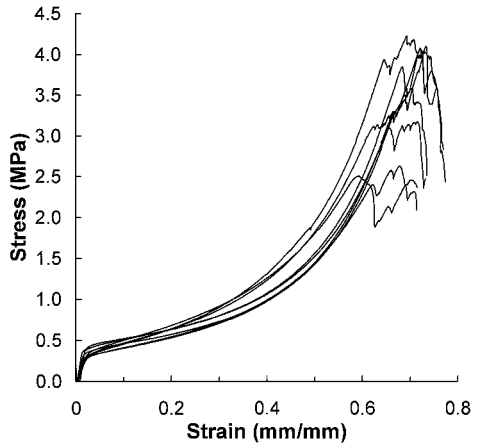

Fig. 7 Stress-strain curves obtained from transverse-compression testing of charred PICA (density = 219 ± 4 kg/m^3).

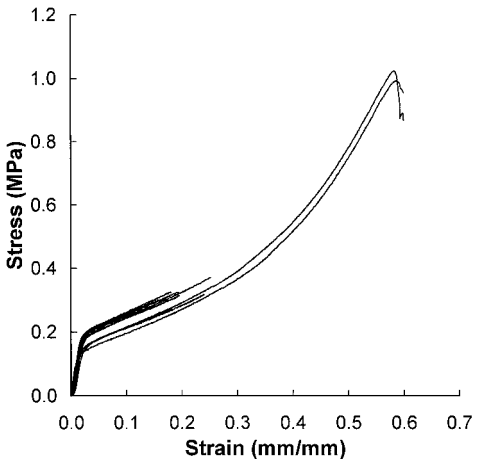

Fig. 8 Stress-strain curves obtained from transverse-compression testing of the Fiberform substrate (density = 185 ± 4 kg/m^3).

curve in Figs. 6–8 corresponds to the stress-strain response of an individual specimen. Only two of the Fiberform specimens in Fig. 8 were loaded to the maximum possible stress. In transverse loading of the materials, the maximum compressive strength S generally occurred simultaneously with macroscopically observed fracture. The values of the initial Young's modulus E_i and yield stress σ_Y are determined from transverse compressive responses in the region of strain less than approximately 0.05, as illustrated in Fig. 9. In particular, E_i is the slope of line segment a in Fig. 9, which is tangent to the stress-strain curve at the point of inflection coincident with

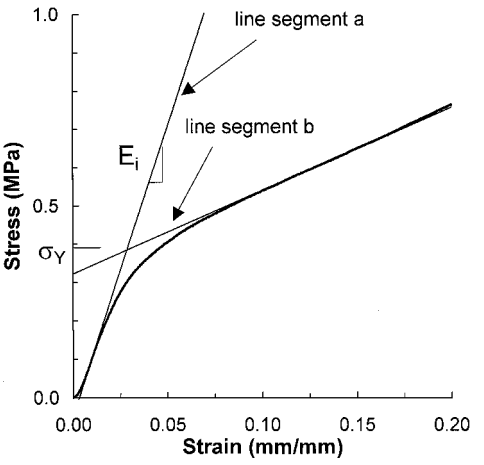

Fig. 9 Typical response of PICA to transverse compression in the domain of relatively small strain and illustration of the method to determine initial Young's modulus E_i and initial yield stress σ_Y.

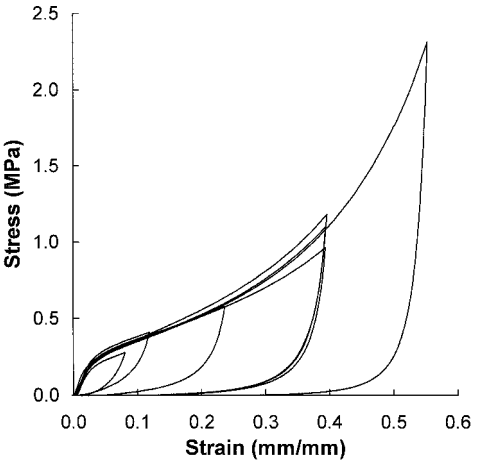

Fig. 10 Hysteresis obtained during transverse-compression testing of PICA. (Each curve is from a different specimen.)

the maximum slope (in the region of strain less than 0.05); σ_Y is the stress at the intersection of line segments a and b, wherein segment b is tangent to the stress-strain curve at the point of inflection coincident with the smallest slope.

To examine hysteresis during transverse loading of PICA, seven PICA specimens, in succession, were loaded to various stress levels that were less than the maximum compressive strength S and then unloaded. The stresses and strains were monitored during both the loading and unloading phases. A new specimen was used for each loading-unloading cycle. Figure 10 shows the results of loading-unloading cycles.

The energy density (i.e., the cumulative energy input per unit reference volume) for representative samples of PICA during transverse compression is plotted vs strain in Fig. 11. The energy density includes energy absorbed during elastic and plastic deformation. It is equal to the area under the stress-strain curve and is given by

$$e(\varepsilon) = \int_0^{\varepsilon} \sigma(\eta)\, \mathrm{d}\eta \tag{2}$$

The results of the hardness testing of the PICA, the charred PICA, and the Fiberform specimens, under the parallel and transverse loading conditions, are summarized in Table 3.

Discussion

Two distinctly different characteristic responses were observed during compression testing. The type of response was determined by the direction of the applied load with respect to the preferred fiber-alignment plane (i.e., parallel, in Figs. 3–5, vs transverse, in Figs. 6–8), rather than by the state of material (i.e., virgin PICA,

Table 3 Hardness of PICA, charred PICA, and the fibrous substrate Fiberform[a]

Material	Density, kg/m^3	Parallel loading		Transverse loading	
		No. of indents	Hardness H, MPa	No. of indents	Hardness H, MPa
PICA	220	15	1.81 ± 0.25	15	1.45 ± 0.17
Charred PICA	225 ± 2	10	1.70 ± 0.20	10	1.01 ± 0.11
Charred PICA	213 ± 8	10	1.73 ± 0.26	10	1.01 ± 0.12
Fiberform	160	7	0.67 ± 0.05	7	0.57 ± 0.04

[a]The values following the $\pm$ are standard deviations; where standard deviations are not listed for densities, a single value of density was determined for one bulk sample.

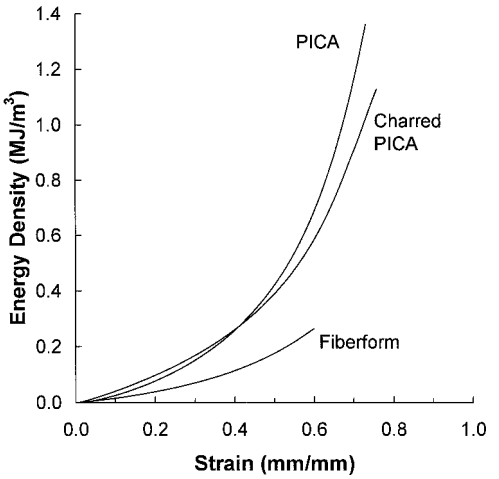

Fig. 11 Energy density vs strain for representative transverse-compression tests on PICA, charred PICA, and Fiberform.

charred PICA, or Fiberform). This result demonstrates the deterministic role of the carbon fibrous substrate in controlling the qualitative features of the compressive behavior. Under parallel loading the compressive responses of PICA, charred PICA, and Fiberform (Figs. 3–5) begin with a steady rise in stress to strains of about 2%; the stress then follows an erratic, somewhat horizontal, path to strains exceeding 5%. This behavior is characteristic of a mainly elastic initial response, followed by irreversible internal buckling of the fibrous substrate and separation of the fibers from each other and/or from the phenolic resin. The materials continue to absorb energy, with increasing strain, as buckling progresses. A similar response was observed by James and Milstein[11] in the parallel compressive response of layered single crystals with covalent in-plane atomic bonding and Van der Waals out-of-plane bonding. In contrast, under transverse loading the responses of PICA, charred PICA, and Fiberform (Figs. 6–8) begin with a relatively linear increase in stress to about 2% strain, after which the slope dramatically decreases and then begins to rise again at an increasingly faster rate up to strains of 60 to 70% where failure occurs. The result is a strongly nonlinear stress-strain curve with upward concavity, i.e., after strains of a few percent the materials become increasingly stiffer as the strain increases. Figure 10 shows that PICA's response under transverse loading exhibits substantial irreversible energy loss after strains of more than a few percent. However, after releasing the load the samples undergo considerable "springback" or recovery toward the initial, unstressed state. The area contained within a hysteresis loop is the energy per (initial) unit volume dissipated during a loading-unloading cycle. This energy can be expended by frictional movement of fibers over each other or through the phenolic resin or possibly by debonding of the fibers from each other or from the resin.

An unusual inverse relation between strength and hardness was observed, i.e., each material exhibits a greater compressive strength in transverse loading, but a greater hardness in parallel loading. Also, each material was more compliant in the transverse hardness tests, as evidenced by smaller slopes of the load-displacement curves (not shown). These hardness test results, although seemingly anomalous at first glance, are fully consistent with the compression results; that is, under parallel compression the materials are initially much stiffer (compare the penultimate columns of Tables 1 and 2), and they reach their maximum stresses at relatively small strains. Furthermore, under transverse loading the materials yield at relatively low stresses (see the last column of Table 2), whereas they fracture at relatively high stresses and large strains. The hardness results evidently reflect the compressive behavior at small or intermediate strains where the compressive stress in parallel loading is higher than the corresponding stress in transverse loading. Therefore, the inverse relation among strength and hardness in the two loading directions is understood.

Although similar qualitative behavior was observed in all compression tests performed with the same loading orientation, there are interesting and revealing quantitative distinctions among the three materials. First, consider just the specimens subjected to parallel loading. For this loading condition the mean compressive strength and hardness values of Fiberform are about 50 and 40% of the corresponding values for PICA, respectively. The lower mean hardness ratio, compared with the mean compressive strength ratio, likely results from the lower density of Fiberform used in the hardness testing (160 kg/m^3) vs that used in the compression testing (187 kg/m^3). The important point, however, is that the phenolic resin accounts for approximately half of the LCA composite's total compressive strength in parallel loading. The resin also contributes significantly to the composite's stiffness, i.e., the secant moduli values in Table 1 of the composite are about three times those of the Fiberform substrate. The behavior of charred PICA is generally intermediate when compared with the corresponding behaviors of PICA and Fiberform, as seen in Tables 1 and 3. The notable exception to this trend is that the average compressive strength of the charred PICA specimens (1.79 ± 0.43 MPa) is appreciably greater than that of the virgin PICA specimens (1.55 ± 0.09 MPa). However, there is considerably more scatter in the charred PICA results, as is evident from Fig. 4 as well as from the indicated standard deviations. If one takes the median value of compressive strength, rather than the mean, both PICA and charred PICA have compressive strengths of about 1.5 MPa. In addition, a portion of the strength of the charred specimens can be attributed to the larger precharred density of the charred specimens relative to the corresponding density of the virgin specimens. In summary, charring causes some degradation of PICA's mechanical properties in parallel loading (including greater variations of compressive strength) but clearly does not cause the behavior to revert to that of the bare Fiberform. Therefore, the char residue also contributes significantly to the strength and stiffness of the composite.

Next, we compare the strength and hardness under parallel loading. Although the stress distribution beneath the spherical indenter during a hardness test on an anisotropic composite material is highly complex, as a first approximation we can assume that a "representative stress" under the indenter at peak load is close to the measured value of the hardness in MPa. Tables 1 and 3 show that hardness values of PICA, charred PICA, and Fiberform in parallel loading are reasonably close to values of compressive strength. This fact suggests that, during parallel hardness testing, there exists highly localized separation and buckling in a small region beneath the indentor (because the dominant mechanism limiting compressive strength appears to be internal separation and buckling). As a result, the present method of measuring the hardness of LCAs

can yield values that correlate well with compressive strengths in parallel loading. However, further testing with a wider variety of LCA materials needs to be carried out to establish any quantitative relationships.

Finally, we compare the behavior of PICA, charred PICA, and Fiberform under transverse loading. As in the case of parallel loading, the transverse mechanical properties of charred PICA tend to be intermediate to the corresponding values for PICA and Fiberform, except in the domain of small strain, where the charred PICA specimens have the greatest average values of initial Young's modulus and yield stress. Also, the phenolic resin provides greater relative strength benefits under transverse loading than under parallel loading. In fact, the compressive strength of PICA is more than five times greater than that of Fiberform in transverse loading but is only about twice as high in parallel loading. Additionally, the compressive strength of Fiberform itself is only about 25% greater in transverse loading than in parallel loading, whereas the strength of the PICA composite is 250% greater in this loading mode. Figure 11 shows that the phenolic resin also greatly enhances the ability of the material to absorb energy during transverse compression, and that charring did not cause large deterioration of this ability.

With regard to possible correlations of strength and hardness under transverse loading, Tables 2 and 3 show that the respective transverse hardness values of each material are well below the transverse compressive strengths and above the initial yield stresses, i.e., the representative stresses exerted by the hardness indenter are in the nonlinear, upwardly concave, regions of the stress-strain curves of Figs. 6–8. Therefore, such stresses are too small to cause significant localized fracture, and in view of the complexity of the stress-strain curves it may be presumed that hardness measurements are unlikely to correlate simply with the corresponding compressive strengths. However, other hardness measuring techniques in which the representative stresses are closer to the compressive strength or to the initial-yield strength may correlate with these properties. This potential for correlation is a topic that needs additional study.

Conclusions

The results from compression and hardness tests on PICA, charred PICA, and PICA's fibrous substrate Fiberform have been presented. The results indicate that the direction of loading, relative to the plane of preferred fiber alignment, rather than the condition of the material, is what determines the nature of the compressive response. When the load is applied parallel to the preferred fiber-alignment plane (parallel loading), PICA, charred PICA, and Fiberform all respond similarly. Initially, the stress increases in a relatively linear manner with strain, for strains up to a few percent, and then the material fails by an apparent internal separation and buckling mechanism. However, the material can continue to support compressive loads for strains well over several percent. In contrast, when these materials are loaded perpendicular to the preferred plane of fiber alignment (transverse loading), the stress increases with strain in a highly nonlinear manner, without signs of failure, for strains exceeding 50%. These results, in turn, imply that the structure of the carbon fibrous substrate, rather than the phenolic or the charred phenolic residue, controls the essential nature of the composites' compressive responses. Addition of phenolic resin to Fiberform causes the compressive strength to increase by factors of about 2 in parallel loading and 5.5 in transverse loading. Thus, the resin provides considerable reinforcement. The mechanical properties of charred PICA are typically intermediate to the corresponding values of virgin PICA and Fiberform. Therefore, the char residue also provides reinforcement. Values of hardness and compressive strength are comparable with each other under parallel loading. However, no simple correlation between these properties is evident for the case of transverse loading, owing to the complex stress-strain response. Typical values of compressive strength range from about 1 to 6 MPa for the materials tested.

Acknowledgments

This work was supported by NASA Grants NAG 2-1148 and NCC 2-1049. The authors wish to thank Kirk Fields, the supervisor of the Materials Testing Laboratory at the University of California at Santa Barbara, for his help in implementing the experiments. The following student assistants are also acknowledged: Joe Mencher, Anthony DiCarlo, Edwin Guerra, Ryan Lotz, Patricia Valenzuela, and Christina Luna.

References

[1]Tran, H. K., "Development of Lightweight Ceramic Ablators and Arc Jet Test Results," NASA TM 108798, Jan. 1994.

[2]Tran, H. K., Johnson, C. E., Hsu, M.-T., Smith, M., Dill, H., and Chen-Jonsson, A., "Qualification of the Forebody Heatshield of the Stardust's Sample Return Capsule," AIAA Paper 97-2482, June 1997.

[3]Tran, H. K., Johnson, C., Rasky, D., Hui, F., Chen, Y.-K., and Hsu, M., "Phenolic Impregnated Carbon Ablators (PICA) for Discovery Class Missions," AIAA Paper 96-1911, June 1996.

[4]Tran, H. K., Johnson, C., Rasky, D., Hui, F., and Hsu, M., "Silicone Impregnated Reusable Ceramic Ablators for Mars Follow-on Missions," AIAA Paper 96-1819, June 1996.

[5]Tran, H. K., Johnson, C. E., Rasky, D. J., Hui, F. C. L., Hsu, M.-T., Chen, T., Chen, Y. K., Paragas, D., and, Kobayashi, L., "Phenolic Impregnated Carbon Ablators (PICA) as Thermal Protection Systems for Discovery Missions," NASA TM 110440, April 1997.

[6]Chen, Y.-K., and Milos, F. S., "Ablation and Thermal Response Program for Spacecraft Heatshield Analysis," AIAA Paper 98-0273, Jan. 1998.

[7]Marschall, J., and Cox, M. E., "Gas Permeability of Lightweight Ceramic Ablators," *Journal of Thermophysics and Heat Transfer*, Vol. 13, No. 3, 1999, pp. 382–384.

[8]Marschall, J., and Milos, F. S., "Gas Permeability of Rigid Fibrous Refractory Insulations," *Journal of Thermophysics and Heat Transfer*, Vol. 12, No. 4, 1998, pp. 528–535.

[9]Kim, K., and Milstein, F., "Relation Between Hardness and Compressive Strength of Polymer Concrete," *Construction and Building Materials*, Vol. 1, No. 4, 1987, pp. 209–214.

[10]Parmenter, K. E., and Milstein, F., "Mechanical Properties of Silica Aerogels," *Journal of Non-Crystalline Solids*, Vol. 223, No. 1, 1998, pp. 179–189.

[11]James, T. W., and Milstein, F., "Plastic Deformation and Dislocation Structure of Single Crystal Mercuric Iodide," *Journal of Materials Science*, Vol. 18, No. 11, 1983, pp. 3249–3258.

M. P. Nemeth
Associate Editor